

Spring 2019

UNH Observatory Exoplanet Transit Depth Limit

Nicholas R. Larose

University of New Hampshire, Durham

Follow this and additional works at: <https://scholars.unh.edu/honors>

Part of the [Instrumentation Commons](#), [Other Astrophysics and Astronomy Commons](#), and the [Stars, Interstellar Medium and the Galaxy Commons](#)

Recommended Citation

Larose, Nicholas R., "UNH Observatory Exoplanet Transit Depth Limit" (2019). *Honors Theses and Capstones*. 455.
<https://scholars.unh.edu/honors/455>

This Senior Thesis is brought to you for free and open access by the Student Scholarship at University of New Hampshire Scholars' Repository. It has been accepted for inclusion in Honors Theses and Capstones by an authorized administrator of University of New Hampshire Scholars' Repository. For more information, please contact nicole.hentz@unh.edu.

UNH Observatory Exoplanet Transit Depth Limit

Nicholas Larose

Advisors: James Ryan and John Gianforte

Department of Physics and Astronomy, University of New Hampshire,
Durham, New Hampshire, 03823 USA

Undergraduate Thesis

May 16, 2019

Abstract

Using the University of New Hampshire Observatory, we performed multiple exoplanet transit observations on a variety of systems. Of these transits, those performed with ideal weather conditions were chosen to do extensive analysis on. The transit chosen for initial analysis was HAT-P-56b. We then used Z-Score values, along with the average mean and standard deviation collected from multiple transits to determine a minimum possible transit depth of 7.4 ± 0.6 mmag. This value will allow UNH to access exoplanet transit databases from survey telescopes and perform follow up observations and / or confirm potential exoplanets, thus making the UNH Observatory more research capable. A follow up threshold transit around 7 mmag will be performed and show that our limit is achievable.

Contents

Introduction	4
Exoplanets	4
Recent Discoveries	5
Methodology	6
Procedure	6
Transit Fitting	8
Analysis	10
Results	13
Appendix	14
Citations / Bibliography	14
Error Analysis	15
Acknowledgments	15

Introduction

Exoplanets

Exoplanets are planets that orbit stars other than our own. The first exoplanet discovered was PSR B1257+12 in 1992 by the Arecibo Radio Observatory, making exoplanet detection a relatively new science[4]. The current number of known exoplanets as of May 2019 is 4,058 according to the Extrasolar Planet Encyclopedia[8]. A common method of detecting exoplanets uses space based survey telescopes such as Kepler and TESS (NASA’s Transiting Exoplanet Survey Telescope) or ground based such as HATnet, which as the name suggests detects a planet by measuring the stellar luminosity before, during and after a transit[4]. The potential exoplanet properties reside in a database, where institutions and amateur astronomers can later access it to confirm and refine the results with independent observations.

Methods developed to detect exoplanets include the radial velocity method, microlensing, astrometry, direct imaging, and planetary transits[16]. For example, the radial velocity method measures the apparent orbital motion of a star as the planet and parent star orbit a common center of mass. Microlensing can detect planets from thousands of light years away, where the light from a far away star passes by another closer star on its way to an observer, bending the light into what is known as an “Einstein Ring” predicted by General Relativity. If the closer star has an orbiting exoplanet, this can cause a measurable increase in brightness of the ring [19]. Direct Imaging is just as the name implies, where by blocking the light from a parent star a direct image of an exoplanet can be taken.

A majority of exoplanets have been discovered via the transit method, which is the same method used for this project[16]. The transit method, as shown in Figure (1) is performed by measuring the brightness of a star as a planet passes in front of it, decreasing the measured flux from our perspective. This dip in brightness allows astronomers to deduce several properties of the planetary system.

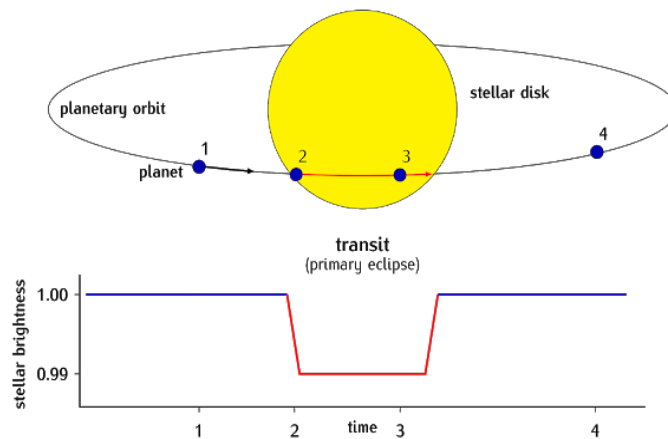


Figure 1: Diagram of an exoplanet transit and example light curve. The plot shows the light flux of the star versus time as the exoplanet passes in front of the parent star.[6]

Since planets are very small relative to their parent star and very far away the reduction in brightness is of order 0.01% to 1% of the stars brightness[16]. It requires clear weather conditions and equipment with a motor drive or autoguider to keep the star in the field of view for the duration of the transit. This means that the larger the planet is relative to its parent star the deeper the transit depth, and the closer it is to the parent star the more frequently the transit occurs. This makes the commonly known “Hot-Jupiters” ideal systems to observe, which are Jupiter sized planets that orbit their star very closely resulting in a short period and also making their surface super heated. These are ideal systems because larger dips in brightness are easier to detect, and night on Earth only lasts about 12 hours, limiting observation time. These systems are most commonly detected, since planets with similar orbital periods to that of Jupiter would require observing the same star for decades.

Transit depths can be influenced by different properties. As explained above, the size of the planet relative to the star can change the depth by blocking a larger amount of the received light. The inclination angle of the exoplanet, which is the apparent angle that the planet passes in front of the star can also change the depth and shape of the light curve. For example, an inclination angle of 90° means the planet passes directly through the center of star relative to an observer. Another factor than can alter the transit depth is limb darkening. This is when the circumference of a star appears darker than the center because light emitted at the “limb” passes through more stellar atmosphere. With all of these factors in mind, the goal of this project is to determine the minimum transit depth, or the smallest drop in brightness of a star that the UNH Observatory can measure. The accuracy of the measured depth depends on the equipment used such as the telescope aperture size, the camera and filters used, and whether or not autoguiding is used. The accuracy and precision of the measurements can also be effected by the weather conditions on the night of observation if a ground based observatory is used.

Recent Discoveries

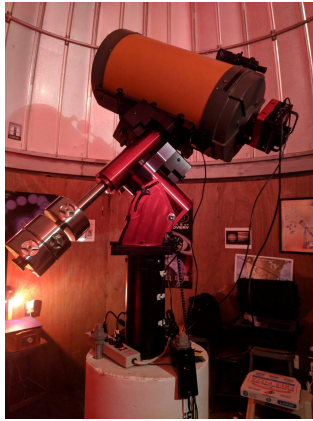
Exoplanet discovery has become an increasingly popular field of study since the first confirmed detection 27 years ago. The rate of discovery has increased tremendously, with 1300 discovered in 2016 compared to about 500 total between the years of 2000 and 2010[8]. As stated previously most of the planets discovered are Jupiter sized, but recently smaller and less massive ones have been detected. The first “Earth-like” exoplanet orbiting in the habitable zone (the region around a star where liquid water can form) was found by Kepler in 2014, designated Kepler-186f. This planet orbits the star Kepler-186 once every 130 days, 500 light years away, and is 1.17 Earth radii in size. The number of potential Earth sized exoplanets in the habitable zone now is over 40.[20][18]

Other recent developments in exoplanetary science include the recent ability to use stellar spectrometry to determine the composition of exoplanets atmospheres. Scientists are also working on methods to detect potential exomoons, or moons orbiting discovered exoplanets, but none has been confirmed yet.

Methodology

Procedure

The objective of this study is to determine the minimum transit depth or the smallest reduction in brightness of a star. As mentioned in Section 1, the exoplanet detection method used at the UNH Observatory is the transit method. This method utilizes the Celestron 14" Schmidt-Cassegrain telescope (C14) mounted on a *Software Bisque Paramount MX+ German Equatorial Mount (GEM)*. The *SBIG STXL-6303E* CCD camera (CCD) is connected to the C14, and both are connected to the observatory computer running *TheSkyX* software, which controls the mount and camera. Shown below in figure (2) is the observatory telescope and camera.



(a) UNH C14 Telescope



(b) SBIG STXL-6303E CCD Camera

Figure 2: UNH Observatory Equipment. The C14 has a 14 inch aperture and a diffraction limited resolution (using a Clear Blue Blocking Exoplanet filter of 500 nanometers) of $\theta = 1.7 \cdot 10^{-6}$ radians or 0.35 arcseconds. The CCD camera has a pixel size of 9x9 microns (10^{-6} meters), and a resolution of 3072 x 2048.[9][13]

Transit data are collected from survey telescopes, and published to databases. We use the Exoplanet Transit Database (ETD[7]) to determine potential transits using the observatory latitude and longitude. A transit is then chosen based on the apparent magnitude of the star, the transit depth, and starting and ending locations in the sky (to ensure its clear visibility, and does not require a meridian swap).

Once a suitable transit is selected, the observatory is prepared at least an hour before the **ingress** (when the edge of the planet first begins to pass in front of the star) in order to set up the equipment. The CCD camera is connected up to the mount and controlled through *TheSkyX* software. First the star field is matched to an example given on the ETD. Based on the brightness of the target star, an exposure time is chosen usually between 30 and 45 seconds. Images are then taken with a 10 second delay between images to allow for field re-centering. The data collection begins thirty to forty five minutes pre-ingress, through the duration of the transit and thirty to forty five minutes post-egress (when the planet leaves the edge of the star).

The data are then transferred from the computer onto a flash drive, and later imported into an image processing/photometry application known as **AstroImageJ** (AIJ). This software is widely used for differential photometry. First, the images are imported from the flash drive into AstroImageJ as .FITS files, which are image files common in astrophotography. The images are then aligned so that all of the stars lie in the same location for the photometry process to work properly.

After they are aligned, the images are run through differential photometry processes. This procedure uses apertures, which are sets of three concentric rings that surround the desired star(s). The first ring captures the desired star entirely, and the region between the outer two apertures are used for the sky background, where the signal is averaged and then subtracted from the source[1]. The recommended radii of these apertures can be optimized by AIJ’s seeing profile as shown below:

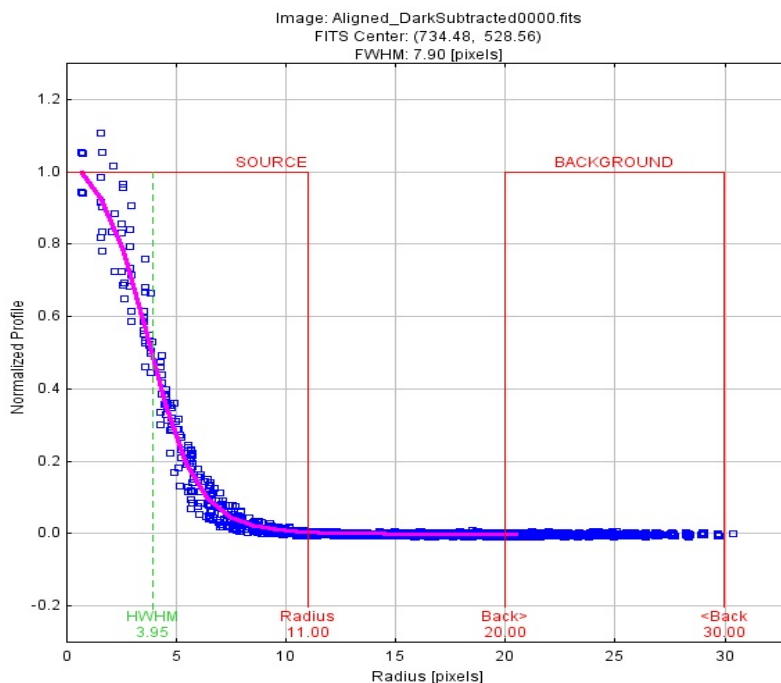


Figure 3: Seeing profile of HAT-P-56 with recommended aperture radii. According to the AIJ user manual [1], “The plot shows the halfwidth at half-maximum (HWHM), the FWHM, and suggested aperture radii in pixels. The aperture radius is set to 1.7FWHM, the inner radius of the sky-background annulus is set to 1.9FWHM, and the outer radius of the sky-background annulus is set to 2.55FWHM” [1].

This process selects a target star (the one being transited in this case) and any number of suitable comparison stars. A suitable star lies in close proximity to the target star, and has a similar apparent magnitude of the comparison star. The number of stars are generally chosen between 2 and 12, and then “turned on and off” post photometric process to optimize the fit, or to minimize the Bayesian Information Criterion (BIC) value (more details in Transit Fitting section).

This process cycles through each of the images, and measures the brightness of the target star relative to that of the comparison stars. The **relative brightness** of the transiting star is calculated as:

$$F_R = \frac{F_T}{\sum_{i=1}^n F_{C_i}} \quad (1)$$

It is important to note that what we are actually measuring is the *intensity* of the star, but in AIJ it is referred to as flux. Where F_T is the flux (or net counts measured in analog-to-digital units, or ADU) of the target star and F_{C_i} is the flux of the n number of comparison stars. The selection of the background region (pre-ingress and post-egress) normalizes the flux to one. The change in flux calculated in the transit fit package of AIJ can be converted to a more commonly used unit in astronomy of **magnitudes** by using:

$$\Delta F_{mag} = -2.5 \cdot \log_{10}\left(\frac{F_T}{F_0}\right)$$

Where F_T is the flux measured during the transit, and F_0 is the flux measured not during the transit. The number 2.5 corresponds to $100^{1/5}$, meaning every 5 magnitude steps the brightness of the object changes by a factor of 100. Using the fact that the flux of an object F_i is equivalent to $Luminosity_i \cdot 4\pi R_i^2$, we can rewrite the change in flux in terms of the planets and stars radii:

$$\begin{aligned} \Delta F_{mag} &= -2.5 \cdot \log_{10}\left(\frac{F_0 - \Delta F}{F_0}\right) \\ &= -2.5 \cdot \log_{10}\left(1 - \frac{\Delta F}{F_0}\right), \text{ where } \frac{\Delta F}{F_0} \ll 1 \\ &= -2.5 \cdot \log_{10}\left(1 - \left(\frac{R_p}{R_*}\right)^2\right) \end{aligned}$$

Where R_p represents the radius of the planet and R_* is the radius of the star[10]. One very important thing to note is that this equation holds true *only* if we assume the star is uniformly bright over the visible disk, i.e. no quadratic limb darkening coefficients. These values take into account the dimming at the edges of the star and is discussed in the Analysis section.

Transit Fitting

With the target star and comparison stars chosen, a normalization region is selected as the regions of background (pre-ingress and post-egress). The software then uses a light curve fitting model to create a fit, which is then refined according to the AIJ user manual stating “the best fit model is found by minimizing χ^2 of the model residuals using the downhill simplex method to find local minima.” [2][15] What this fit does is model the transit as an eclipse of a spherical star by an opaque planetary sphere[1].

The fit mode in AIJ takes in the transit duration and size of the star (in R_{Sun}), whose values are taken from **The Extrasolar Planet Encyclopedia**[8]. The application then

models a transit fit that can be modified by detrend parameters, transit inclination and quadratic limb darkening values. The main goal of modifying these values is to get the most accurate fit, meaning getting the $\chi^2/(df)$ as close to 1 as possible, and to get Bayesian Information Criterion, or BIC value as low as possible. This value is defined as:

$$\text{BIC} = \chi^2 + (\text{number of fitted parameters}) * \ln(\text{number of data points})$$

As stated in AIJ, the fit with the lowest BIC indicates the preferred model.[1] After AIJ determines the best fit with the chosen parameters, it estimates the planetary radius to calculate the transit depth in ADU. We then use the above equation to convert that to the more useful unit of magnitudes. The transit fit for HAT-P-56b performed on (1/31/2019) is shown below:

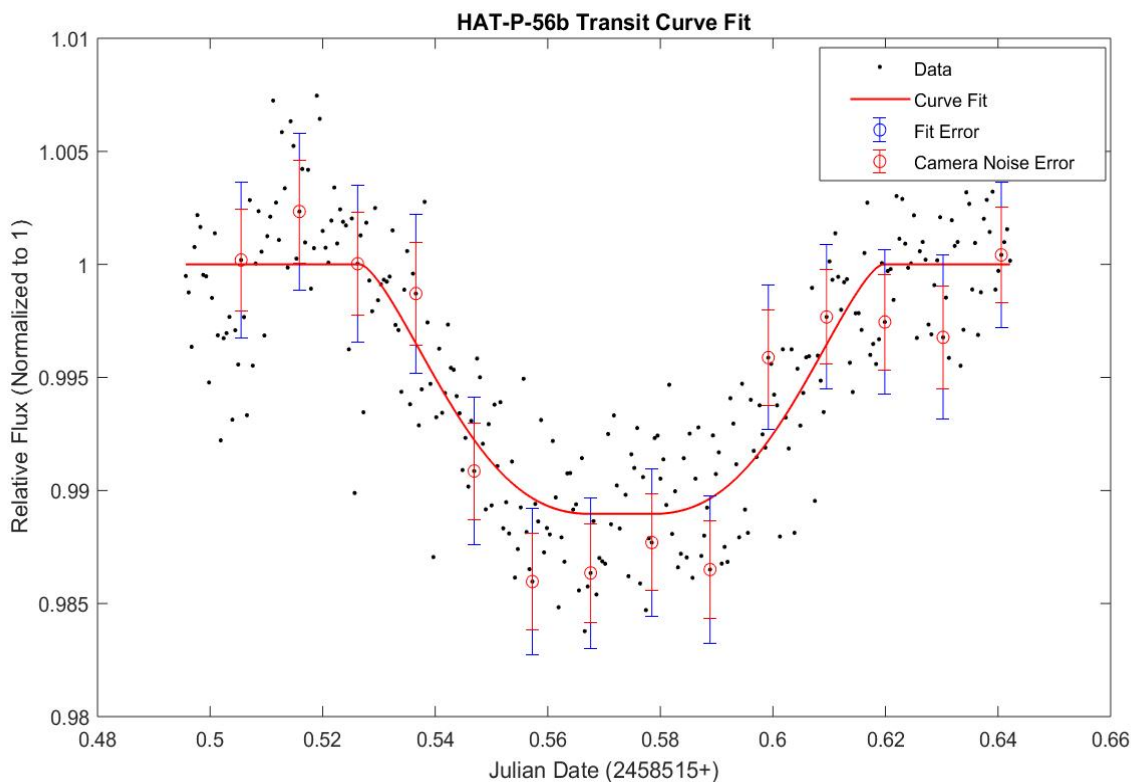


Figure 4: Plot for HAT-P-56b including AIJ optimized curve fit and error bars from camera noise and fit procedure. The individual photometric data points are shown as black dots, however a sampling of those points is represented as red circles with their associated errors so the scatter in the data point can be compared to the intrinsic error in each measurement. The spread of the data has a standard deviation of 0.0028 ADU.

Julian Date is the time axis. For reference, the data collection period for this particular transit is 3.5 hours. The Camera Noise Error is the noise contributions from the measurement of a point source using CCD aperture photometry, which is required for photometric error calculations. The computer model of a ‘‘CCD Equation’’ was developed by Merline & Howell (1995) to estimate the signal to noise ratio of a measurement and is described in the Appendix as equation (4). The Fit Error is the difference from each data point to the curve fit, where not every error bar comes into contact because of systematic error. Using the following parameters:

- Orbital Period: 2.7908327 days
- Radius of parent star: 1.428 R_{\odot}
- Inclination Angle: 88.8°
- Quad LD u_1/u_2 : 0.3692

The transit fit was calculated with a χ^2/df of 0.974, shown above in Figure 4. The transit depth using this fit was 0.0112 ADU, which using the unit conversion equation is equal to 12.23 mmag. Since the accepted value on the ETD is 12.0 mmag, the experimental error for this transit is 2%.

Analysis

Our goal in performing the analysis on these transits was to determine the smallest reduction in brightness that we could deem statistically significant. This involved using hypothesis testing and Z-Score (number of standard deviations from the mean) calculations. To begin analysis, it was first noted that the data held a Gaussian structure. That is, we could analyze our data following a normal distribution, making the overarching question one of statistical significance[11].

The analysis for this portion of the thesis was chosen to be **HAT-P-56b** from the HATnet survey. This transit was chosen because it was performed on a night with good seeing conditions. This means it was performed with little to no cloud cover, no lunar interference, high altitude transit requiring no meridian swap, low temperatures, humidity and wind speeds. The data for that night is listed below:

Weather Condition	Low	High
Altitude(Direction)	60° E	75° S
Temperature	0°F	6°F
Humidity	31%	37%
Wind Speed	7 MPH	13 MPH

Table 1: Weather conditions for the duration of the transit for HAT-P-56b performed on January 31, 2019. The altitude and direction is that of the target star. The transit began at 60° E and ended at 75° S. The moon phase was a waning crescent and did not rise until 3:50 am, well after the post-egress data was collected.

The first step in this process is determining whether there *is* a transit present. This requires hypothesis testing, which involves statistically determining if a hypothesis is true or not. We formed a null hypothesis (H_0) which we want to disprove, and an alternate hypothesis (H_A) that is resorted to if the null hypothesis is disproved. The null hypothesis in this case states: *There is no transit present.* This makes the alternate hypothesis: *There is a transit present.* It is important to first determine whether there even is a transit to take measurements of in the first place. Although transits are found from predictions on the ETD, and the transit is usually confined between predicted ingress and egress times, there needs to be certainty. Once it is determined that the intensity drop observed in the eclipsing time period is statistically significant, we can continue. In order to do this, we utilized Z-Scores. These values can be used to determine the probability of measuring the transit depth based on the data population mean and standard deviation. The Z-Score is defined as:

$$Z = \frac{|x - \mu|}{\sigma} \quad (2)$$

Where x in our case is the transit depth, μ is the population mean and σ is the population standard deviation. The population mean and standard deviation values are calculated from the residuals, which is the difference between the measured value and the fit.

After the transit depth is estimated in AIJ, the data is exported into Atom (text editor), where a script written in python calculates the standard deviation and population mean for this particular data set. Once these values are obtained, a Z-Score of 3.57 is calculated. For reference, using a standard confidence value of 95% and a Z-Score of 3.0, the probability of measuring that signal is 0.01%. This means that the probability of measuring the above transit depth given the standard deviation and population mean is $< 0.01\%$, making this transit **statistically significant**. This therefore voids the null hypothesis and proves a transit is present. This lays the framework for how the minimum transit depth will be calculated. Averaging the standard deviation and population means from multiple transit performed with the same UNH equipment gives us a more accurate statistical spread. These transits needed to be performed on nights with similar conditions as described above, since the minimum transit depth will only be able to be observed on those nights, where the statistical spread due to atmospheric conditions is minimized.

We then needed another transit to select to average the aforementioned values. Out of the ten observed transits over the last two years, WASP-10b (performed on 11/29/2018) was the only other one observed in its entirety on a night with optimal seeing conditions and a well defined depth. This transit observation went through the same procedure as HAT-P-56b, giving a χ^2/df of 0.928. This transit was also deemed statistically significant with a Z-Score of 7.99. This high value is due to the transit depth of 35.4 mmag. The accepted value for this transit from the ETD is 39.4 mmag, giving an experimental error of 10%.

The plot of WASP-10b with the corresponding fit is shown below:

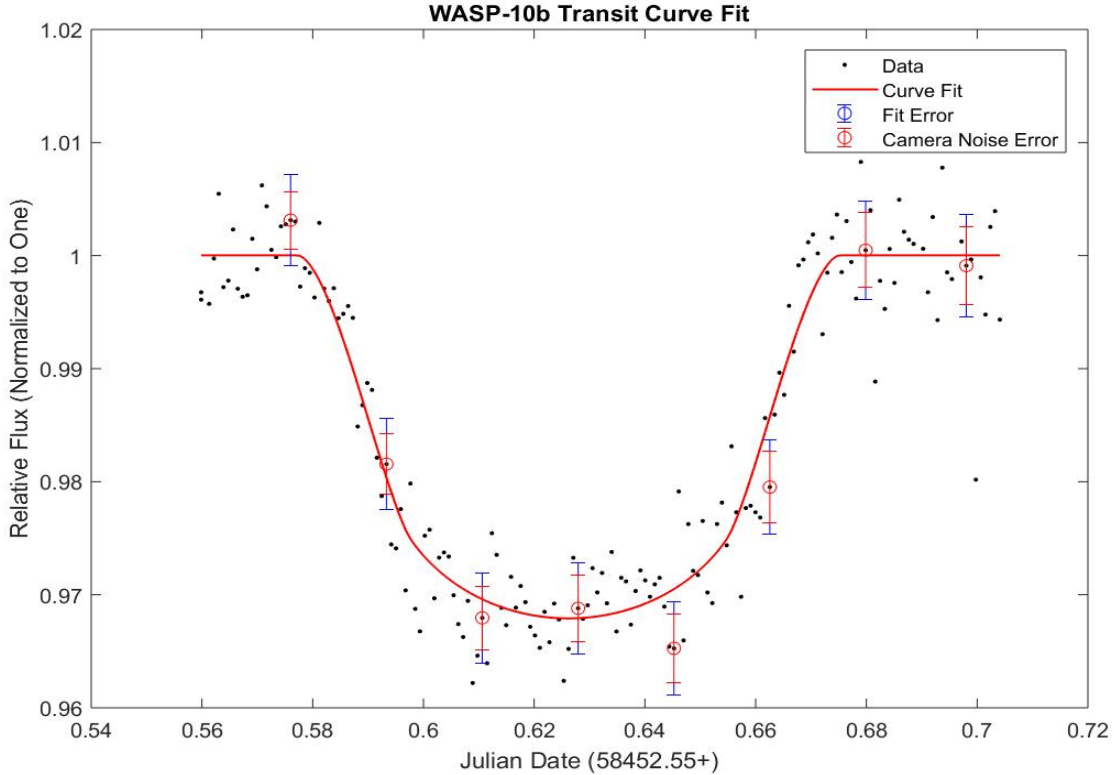


Figure 5: Plot for WASP-10b including AIJ optimized curve fit and error bars from camera noise and fit procedure. Again, only every twenty error bars are displayed for visual purposes. The spread of the data has a standard deviation of 0.0039 ADU.

We then needed to choose a Z-Score, or the smallest number of standard deviations from the mean for a transit can still be deemed significant. For example, choosing a value of 3σ would place the probability of a measured transit being due to random data spread at about 0.3%, *but* using the mean and standard deviation from HAT-P-56b this puts the minimum depth at 12.07 mmag, which we have already proven to be a measurable transit from HAT-P-56b. Values as low as 1σ give too low probabilities, placing the probability of a transit being due to error at almost 30%. It was decided to choose a Z-Score of 1.7σ , a reasonable middle ground giving the probability of a transit being faulty of around 10%.

There are two ways to determine the transit depth after a fit is calculated. The first more approximate way of determining the transit depth is assuming the star has uniform brightness, or setting what is known as the quadratic limb darkening coefficients to zero. These values denoted in AIJ as Quad LD u1 & u2 take into account that stars are not uniformly lit, and the intensity decreases as one looks towards the edge of a star, or its “limb”, and range from zero to one[16]. This is due to light having to travel through more of the stars atmosphere before reaching an observer. These values can cause transit fits to deepen and/or

narrow, changing the values of the calculated transit depth. These values can be found on databases, from research tables or can be calculated online at EXOFAST[21]. These values are important in estimating the transit depth and without using them can lead to errors of a few mmag. For example, the difference of limb darkening coefficients from zero to one for WASP-10b changed the estimated depth by about 4 mmag.

Results

The goal of this project was to determine the minimum exoplanet transit depth that the UNH Observatory is capable of. This was accomplished by performing multiple exoplanet transit observations over the course of my junior and senior years. The data collected went through a photometry program AIJ to obtain light curves. We then used AIJ to estimate the transit depth, and using statistical analysis we deemed whether the transit was statistically significant or due to error. We could then determine how significant it was with Z-Scores, which we then used to determine the minimum transit depth. After collecting the results from the two transit HAT-P-56b and WASP-10b, and using the chosen Z-Score of 1.7σ , we were able to statistically determine a minimum exoplanetary depth of **7.4 ± 0.6 mmag**.

This is not enough to observe earth sized exoplanets since their decrease in brightness relative to their parents star is much smaller, but can observe other confirmed planets such as HAT-P-49b or WASP-90b (ETD). For example HAT-P-49b is a hot-jupiter at $1.4 R_J$ and orbits its star at 0.044 Astronomical Units (AU) every 2.7 days[8]. As stated before, this minimum transit value makes the observatory more research capable by allowing the University to perform followup observations of candidate systems discovered by others.

Other projects being performed by Tom Ireland and Anthony Cappuccio are attempting to integrate autoguiding to the CCD camera / mount, and to use full image calibration to improve the quality of data collected in transit observations. Autoguiding will allow the telescope to track a star throughout the entirety of the transit without needing to adjust the frame. This will also allow the stars to stay on the same pixels of the sensor during the transit, decreasing the noise collected throughout. Flat frame subtraction will increase image quality, for example by removing optical vignetting and other imperfections in the optical path. These contributions will contribute to the UNH Observatory by making it more research capable and decreasing the transit depth limit.

Appendix

Citations / Bibliography

- [1] Collins, Karen A., et al. “Astroimagej: Image Processing And Photometric Extraction For Ultra-Precise Astronomical Light Curves. *The Astronomical Journal*, vol. 153, no. 2, 2017, p. 77., doi:10.3847/1538-3881/153/2/77.
- [2] Nelder, J. A., & Mead, R. 1965, *The Computer Journal* 17, 308
- [3] Collins, Karen. Transit Fitting plus Referencing Software in Paper. *AstroImageJ, 2AD*.
- [4] *The Habitable Exoplanets Catalog*. Planetary Habitability Laboratory @ UPR Arcibo, (2018)
- [5] “*Links to Data in the Exoplanet Archive*. Data Resources in the Exoplanet Archive. NASA (2019)
- [6] *Exoplanet Diagrams*. The Transit Method, 1 Jan. 1970 (2018)
- [7] *Exoplanet Transit Database*
- [8] *The Extrasolar Planet Encyclopedia*
- [9] “*STXL-6303E*. Diffraction Limited. Specifications (2019)
- [10] “*Magnitudes and Distances*” Astro Wku. (2019)
- [11] “*Tests of Significance*. Tests of Significance, Yale.
- [12] Seager, S., and G. MallenOrnelas. A Unique Solution of Planet and Star Parameters from an Extrasolar Planet Transit Light Curve. *The Astrophysical Journal*, vol. 585, no. 2, 2003, pp. 10381055., doi:10.1086/346105.
- [13] Pereyra, Antonio, et al. “Characterizing a CCD Detector for Astronomical Purposes: OAUNI Project. *Revista Científica TECNIA*, vol. 26, no. 2, 2017, p. 20., doi:10.21754/tecnia.v26i2.54.
- [14] “AstroImageJ 2.4.1 User Guide plus Getting Started with Differential Photometry.
- [15] Mandel, K., & Agol, E. 2002, *ApJ*, 580, L171
- [16] Wilson, Paul. “The Exoplanet Transit Method. PaulAnthonyWilsoncom, 2015, Exoplanet Detection Techniques
- [17] AstroImageJ, (2019), Photometry & Image Processing Application.
- [18] Schneider, J. “Interactive Extra-solar Planets Catalog”. *The Extrasolar Planets Encyclopedia*. Retrieved 1 May 2019.
- [19] Microlensing. *The Planetary Society Blog*, The Planetary Society.
- [20] Culler, Jessica. Kepler Finds 1st Earth-Size Planet In ‘Habitable Zone’ of Another Star. NASA, 24 Mar. 2015.
- [21] Eastman, et al. *EXOFAST*, 2013

Error Analysis

The Error was calculated in AIJ according to the AIJ manual by combining the noise of each aperture in quadrature to give a total noise of:

$$N_E = \sqrt{\sum_{i=1}^n N_{C_i}^2} \quad (3)$$

Where i indexes the comparison stars, n is the number of comparison stars and N_{C_i} is the noise for each comparison star as calculated by:

$$N = \frac{\sqrt{GF_* + n_{pix}(1 + \frac{n_{pix}}{n_b})(GF_S + F_D + F_R^2 + G^2\sigma_f^2)}}{G} \quad (4)$$

where according to the manual “ G is the gain of the CCD in electrons/ADU, F is the net (background subtracted) integrated counts in the aperture in ADU, n_{pix} is the number of pixels in the aperture, n_b is the number of pixels in the region used to estimate sky background, F_S is the number of sky background counts per pixel in ADU, F_D is the total dark counts per pixel in electrons, F_R is read noise in electrons/pixel/read, and f is the standard deviation of the fractional count lost to digitization in a single 12 pixel ($f \approx 0.289$ ADU for f uniformly distributed between 0.5 and 0.5).” [1]

Error is then propagated through the relative flux to find the flux error as:

$$\sigma_{relflux} = \frac{F_T}{F_E} \sqrt{\frac{N_T^2}{F_T^2} + \frac{N_E^2}{F_E^2}} \quad (5)$$

Where F_T is the net integrated counts from the target star, F_E is the net counts from comparison stars, N_T is the noise of the target star and N_E is the total noise of the comparison stars both according to the above noise equation (4).

Acknowledgments

I would like to thank UNH Observatory Director John Gianforte and my academic advisor Professor James Ryan in assisting me in the processes and completion of this project over the course of my Junior and Senior years, and gaining invaluable experience with observational astronomy and data analysis. I would also like to thank Thomas Manion, Brian O’Conner, and Emma Clarke in assisting me in data collection for a number of these transits, as well as Anthony Cappuccio and Thomas Ireland in their contributions to the Observatory.